

# Dynamic Inertia Response Support by Energy Storage System with Renewable Energy Integration Substation

Yeuntae Yoo, Seungmin Jung, and Gilsoo Jang

**Abstract**—In recent years, the expansion of renewable energy in electric power systems has been increasing at such a rapid pace that it has started affecting frequency stability. Renewable generators connected to the grid produce variable amounts of power, and in most cases have no inherent inertia response (IR) to the system frequency. Therefore, the high penetration of renewable generators in the system results in low inertia and frequency distortion. If renewable generators account for a high proportion of the supply in a power system, the use of energy storage systems (ESSs) with frequency-support algorithms (in the place of synchronous generators) can stabilize the network. The participation of ESSs in frequency support must be organized precisely, so that they are fully devoted to their own purpose. In this paper, the frequency-support parameters of ESSs are calculated for achieving stable frequency response from a network. An estimation and calibration process is conducted during the active power-order change of the ESSs in the substation, and is verified through electromagnetic-transients-including-DC (EMTDC)-based simulations.

**Index Terms**—Energy storage system (ESS), frequency response, inertia, renewable energy substation.

## I. INTRODUCTION

IN recent years, the installed capacities of wind and photovoltaic (PV) generation have been increasing globally because of environmental and economic concerns. Europe, and a portion of North America, have already reached a significant level of renewable energy penetration. Other developing countries have also shown progress in terms of deploying renewable generators in their power system sectors [1].

Owing to the variability of renewable generation output, the planning and balancing of a power system by transmission system operators (TSOs) have become more complex. For system planning, operators must examine short- and long-term adequacy studies, considering various weather con-

ditions. This means that some variability of wind and PV power production should be considered in the studies, with different time scales. Long-term variations may last from 4 to 12 h, and these variations can be balanced using the forecast information [2]. Under extreme weather conditions (such as storm or cloud cover), renewable power production changes rapidly. More than 80% of the production capacity can be reduced in less than 6 h [2].

The increasing use of renewable generators in power systems results in the displacement of conventional synchronous generators. The displacement of synchronous generators reduces frequency stability of the network, as most of the renewable generators do not have inherent inertia or a primary frequency response [3]. As the participation of renewable generators in the grid increases, the fluctuations of frequency in power system also increase, owing to the lack of inertia and frequency response. Because the output of the renewable generators depends on the environmental state, it requires additional reserves to balance the supply and demand when the renewable energy production is expected to result in a surplus. To integrate large renewable generation output and secure reliability of the grid, several constraints and compensation schemes have been introduced.

Curtailing renewable generation output is still the most reliable and commonly used reliability countermeasure applied in power systems. The advanced features of this option have been utilized in various countries with high renewable participation levels. In the Nordic grid code, wind turbines provide the primary reserve by adopting power production limits and ramp rate limits for their production [4]. In [3], [5], [6], wind turbine curtailment is applied to provide a primary frequency reserve for the network. However, the curtailment of renewable generation is not a desirable operation strategy for renewable generators from the viewpoint of system efficiency.

The synthetic inertia response (IR) from renewable generators is another frequency-support strategy used in networks with high wind power participation [7]. In a contingency situation, especially during a short supply of active power, wind turbines can provide extra power to a network above its maximum power-extracting operation point. In [8], [9], a novel IR control strategy using doubly-fed induction generator (DFIG)-type and permanent magnet synchronous generator (PMSG)-type wind turbines is introduced. The IR from

Manuscript received: November 12, 2018; accepted: May 9, 2019. Date of CrossCheck: May 9, 2019. Date of online publication: November 4, 2019.

This work was supported by the framework of international cooperation programs managed by the National Research Foundation of Korea (No. 2017K1A4A3013579) and the Korea Institute of Energy Technology Evaluation and Planning (KETEP) grant funded by the Korea government (MOTIE) (No. 20183010025440).

Y. Yoo and G. Jang (corresponding author) are with Korea University, Seoul, Korea (e-mail: yooynt@korea.ac.kr; gjang@korea.ac.kr).

S. Jung is with Hanbat National University, Daejeon, Korea (e-mail: seungminj@hanbat.ac.kr).

DOI: 10.35833/MPCE.2018.000760



wind turbines is efficient, in which the frequency deviation decreases without the support from synchronous generators; however, it is not sufficient as a primary frequency reserve. In fact, extracting surplus power from wind turbines exacerbates the recovery of frequency after a contingency occurs in a system, as wind turbines have low power-harnessing efficiency when their operation point deviates from the normal position.

For the maximum utilization of renewable sources, additional reserves must be prepared using energy storage systems (ESSs) such as pumped hydro system and battery energy storage system (BESS) [10]. Both these sources are adequate for providing fast and reliable primary frequency response. In particular, the use of a flywheel and BESS can provide a response fast enough to minimize frequency deviations during normal operation, or when in a contingency situation. The use of the BESS to provide inertia and primary frequency response is introduced in [10]. An adequate capacity of BESS could provide sufficient frequency reserves in a power system when only a few synchronous generators are online.

When installing renewable generators into a grid, cost is an important factor that determines the sizes of the facilities. The enlargement of wind and PV farm sizes is a recent trend observed in renewable industries. When interconnecting large offshore wind turbines to the main grid, a significant base cost is incurred for facilities such as connection cables and offshore and onshore substations. Unlike small-scale distributed renewable generators, large wind or PV farms are obligated to apply strict grid codes, considering their influence on the power system. In the cases of interconnection, a point of common coupling (PCC) of a wind or PV farm is a point where the assessments of influence by generation of those sources on the system are conducted. For this reason, ESSs are often installed at PCCs to smooth out variations in output power and time shifting, and to either store surplus wind energy during low-demand periods or discharge energy during high-demand periods. In the Korean power system, ESS-mounted modular substations have been developed for the integration of renewable generators. These ESS substations will be implemented at places where the installation of renewable generators is expected to increase significantly.

For now, most ESS installation is oriented toward the time shifting of production rather than toward supporting the integration of renewable generators and grids [11]. By assessing the frequency-support capabilities of the ESS in real time, the penetration-level limitations of renewable generation are expected to expand. In this paper, an online assessment of the frequency reserve in a power system is proposed to optimize the operation of an ESS in a given power system. The synthetic inertia and primary frequency-response parameters of the ESS are determined according to the operational margin of the ESS. The ESS considered in this paper is originally scheduled to help smooth out the operation of a wind farm. The network stability is assessed, and the frequency-support parameters of the ESS are calculated each time the ESS changes its operation. The proposed algorithm could minimize the participation of ESS frequency support without

endangering the frequency stability of the system.

## II. ESS SUPPORT METHODOLOGIES

### A. Frequency Response Characteristics for Stability Assessment

The frequency of a power system is directly related to the balance between supply and demand of active power in the network. The lack of supply or demand leads to a frequency change as a result of the imbalance between the mechanical and electrical power of the generators. Load demand varies with time, and it has served as a major driving factor of frequency deviation in previous power systems. By contrast, in a modern power system, renewable generators are primarily considered in the dispatch process of other generators to balance the network.

The relationship between active power change and frequency deviation can be explained by the inertia and governor droop constant ( $R$ ) of the synchronous generators in the system. In a contingency situation such as a large generator trip, load shedding, or a transmission line trip, the frequency changes rapidly until the imbalance between the supply and demand is cancelled. Synchronous generators in the grid release kinetic energy from their rotating masses until they achieve a new synchronous speed. The relationship between rates of frequency change and generator inertia is defined [12] as follows:

$$\frac{df}{dt} \frac{2H_{sys}}{f_0} = \frac{\Delta P}{S_{sys}} \quad (1)$$

where  $S_{sys}$  is the capacity of the online generators;  $\Delta P$  is the power imbalance or active power output change from the generators;  $f_0$  is the initial frequency following the input-output imbalance in active power; and  $H_{sys}$  is the equivalent inertia constant of the power system. It should be noted that nonsynchronous generators such as wind turbine, PV, and ESS are not included in the calculation of  $S_{sys}$ . To make the wind turbines and PV contribute to the IR, an additional control system is required to override the control order of active power that follows the operation point with maximum efficiency.  $H_{sys}$  is defined as:

$$H_{sys} = \frac{\sum_{i=1}^N H_i S_i}{S_{sys}} \quad (2)$$

where  $N$  is the number of generators;  $S_i$  is the rated capacity of the individual generators; and  $H_i$  is the inertia constant of each generator. By substituting (2) into (1), the rate of change of frequency (ROCOF) can be defined as:

$$\frac{df}{dt} = \frac{\Delta P f_0}{2 \sum_{i=1}^N H_i S_i} \quad (3)$$

After the contingency situation is resolved and the system reaches a new steady state, several generator outputs change, and the individual generator output is determined by the governor droop constant. Unlike the IR, governor response is proportional to the deviation of frequency value. The relationship between the frequency and generator output is defined

as:

$$\Delta P_{GEN} = \frac{\Delta f S_{GEN}}{f_{nom} R} \quad (4)$$

where  $f_{nom}$  represents the nominal frequency of the system and  $S_{GEN}$  represents the total capacity of generators in the system. In a power system with multiple generators, the equivalent sum of each governor droop constant should be considered. The frequency and governor response in a multi-generator network is generally defined as:

$$\Delta f_{ss} = \frac{\Delta P}{\sum_{i=1}^N \frac{1}{R_i} \frac{S_i}{f_0}} \quad (5)$$

where  $\Delta f_{ss}$  is the deviation of the steady-state frequency when a mismatch of  $\Delta P$  is induced in the network; and  $R_i$  is the droop constant of generator  $i$ .

The characteristics of frequency response can be explained using (3) and (5), and the general behavior of the grid frequency response is depicted in Fig. 1, where SOC represents state of charge.

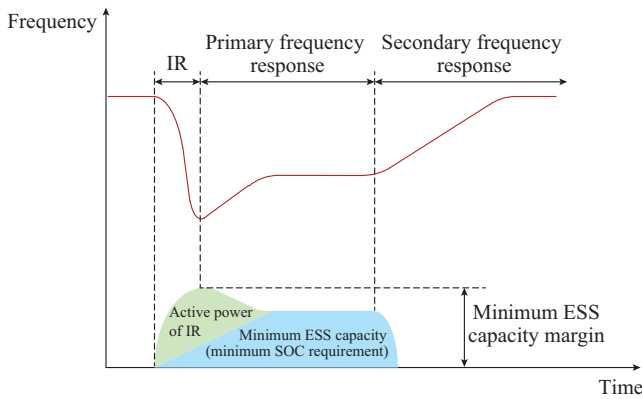


Fig. 1. Characteristics of frequency response.

The frequency drop after a power loss  $P_{loss}$  is arrested when the sum of IR and governor response matches  $P_{loss}$ . If the ramp up of the generator output is not sufficiently fast, or if the generator reserves are depleted, the system state would drive the frequency down to the load-shedding point. In this respect, the ROCOF is an important parameter for assessing the characteristics of frequency response of the grid. In normal operation, a small change in the load demand or renewable generation output can be mitigated if enough grid inertia and system capacity exist. As the increasing participation of renewable generation displaces the synchronous generators, the inertia and system capacity will decrease to dangerous levels [11]. Therefore, certain grid codes such as the European grid code (ENTSO-E) include an ROCOF capability assessment for DC application [13]. A proposed standard of ROCOF of power system for the reliable operation of the grid is 0.5 Hz/s [14].

As shown in Fig. 1, the ESS can supply an IR and primary frequency response in case of emergency. In the following section, the methodology of the frequency-support assessment of ESS in real-time operation is presented.

### B. Methodology for Online Reliability Assessment

The integration of renewable generators into a grid requires a PCC station, which usually includes a step-up transformer and measuring devices. The main purpose of ESS installation at this point is to conduct smoothing and time shifting of the renewable generation output.

Figure 2 shows the operation strategy and topology of the ESS, where LVRT represents low voltage ride through,  $P$  is the active power output,  $S_{ESS,margin}$  is the remaining capacity of the power conversion system (PCS) of ESS to its rated values, and  $P_{ESS,ref}$  is the reference order of active power for ESS. In normal operation, the ESS performs output smoothing by following the set points of the grid operator in consideration of the demand and weather forecasting information. Considering the variability of the renewable generators, the smoothing-out order change takes place every 15 min. At every operation step, the ESS output change will derive a small frequency change in the network. By measuring the frequency and calculating the rate of change during operation, the system inertia parameters can be assumed from (3) for the assessment of grid reliability.

The measured frequency needs to be filtered in order to calculate ROCOF, as the direct differentiation of measured frequency can be noisy. In this paper, the discrete least-squares approximation of frequency is used, rather than direct filtering. Direct filtering may contain oscillatory components produced by synchronous generators [15]. The sampling period is 0.03 s, and 10 points of data are aggregated for approximation. The ROCOF of the measured frequency is defined as:

$$a_1 = \frac{n \sum_{i=1}^n y_i x_i - \sum_{i=1}^n x_i \sum_{i=1}^n y_i}{n \sum_{i=1}^n x_i^2 - \left( \sum_{i=1}^n x_i \right)^2} \quad (6)$$

where  $n$  is the number of sampling data; and  $x_i$  and  $y_i$  are the time and frequency values, respectively. Using (6), a given set of discrete frequency points can be approximated using an algebraic polynomial equation, as follows:

$$f = a_0 + a_1 t \quad (7)$$

where  $a_0$  is the measured frequency at the moment when frequency is sampled, and  $a_1$  becomes ROCOF at that moment. By rearranging (3), we obtain

$$\sum_{i=1}^N H_i S_i = \frac{\Delta P f_0}{2 \frac{df}{dt}} \quad (8)$$

In (8), all terms on the right-hand side are known values, as the active power order for the ESS substation is planned in advance based on the renewable forecasting information. Thus, the current value can be determined as the sum of all products of  $H_i$  and  $S_i$  by measuring the ROCOF. Based on (8), the sums of all products of each  $H_i$  and  $S_i$  are directly related to the ROCOF of the system when the balance between the input and output of active power is lost.

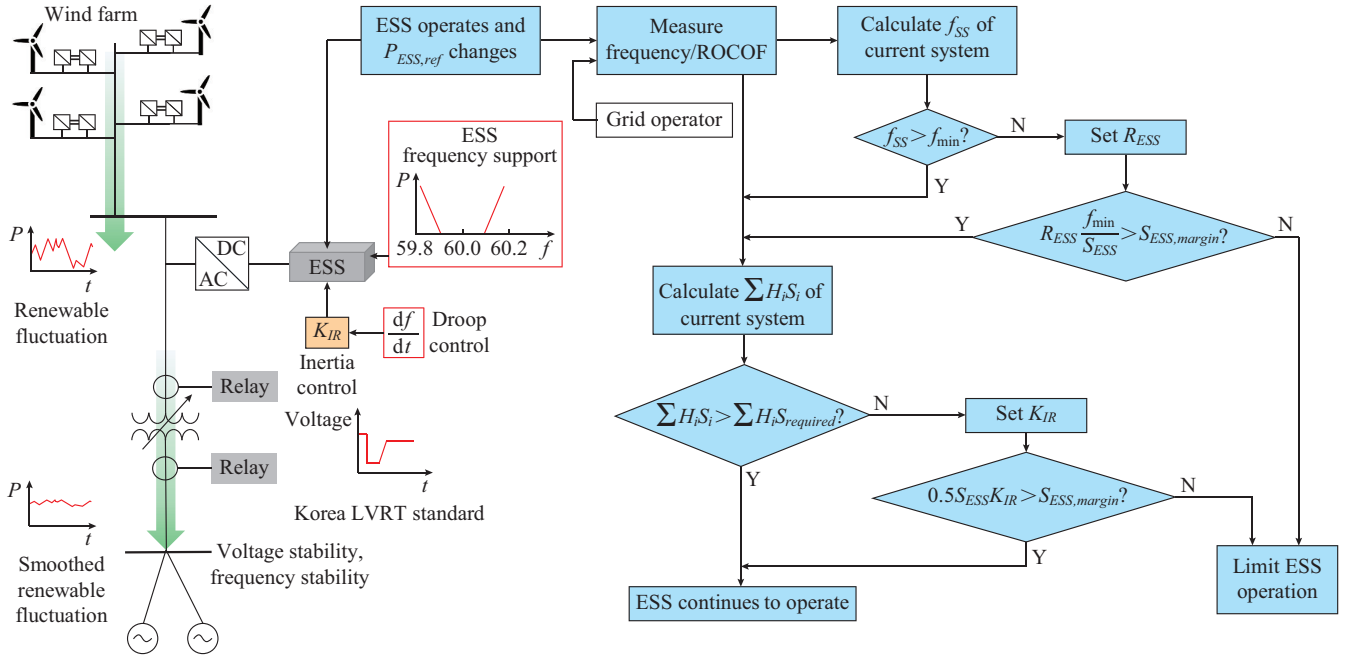


Fig. 2. Operation strategy of ESS for wind farm interconnection.

Thus, assuming that the ROCOF of a stable power system does not exceed 0.5 Hz/s, the minimum requirement of the total products of  $H_i$  and  $S_i$  can be calculated using (8). In this case,  $\Delta P$  represents the capacity of the largest generator in the given system, and can be used to consider the largest imbalance of active power that could be lost in the network.

### C. Optimal Parameters for ESS

The ESS can emulate the IR by implementing active power control, the value of which is proportional to the ROCOF, as depicted in Fig. 3, where  $P_{ESS,nom}$  is the original order of active power for ESS. Using the inertia control strategy, the ESS can have IR and thus, the entire system frequency response can change along with the ESS parameters.

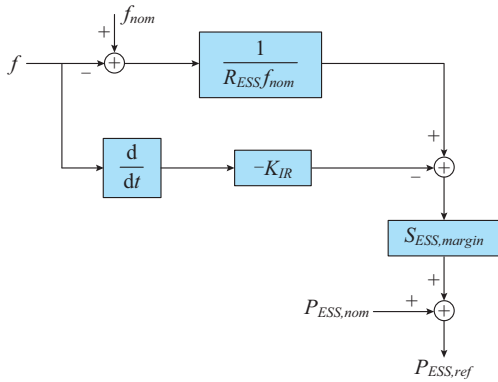


Fig. 3. Frequency-support operation of ESS.

In addition, the ESS can also have an active power-control loop, which can be used to generate an output proportional to the change in frequency. This is identical to the governor response of synchronous generators. Using (5) and

(8), the optimal droop constant of ESS ( $R_{ESS}$ ) and gain of IR values ( $K_{IR}$ ) for the ESS can be calculated, as shown in Fig. 2. The emulated inertia time constant is defined in [10] as:

$$H_{ESS} = K_{IR} \frac{f_0}{2} \quad (9)$$

In [16], maintaining ROCOF within  $\pm 0.5$  Hz/s is recommended to ensure the reliable operation of the power system. To validate the proposed algorithm, the above ROCOF standard is used as a reference in this paper. Using (8), (9) and the maximum limit of the ROCOF value, the minimum ESS IR parameter can be designated as:

$$\sum_{i=1}^m H_{ESS,i} S_{ESS,i} \geq \frac{\Delta P_{\max} f_0}{2 \frac{df_{\max}}{dt}} - \sum_{i=1}^N H_i S_i \quad (10)$$

where  $m$  is the number of ESS substations in the network;  $f_{\max}$  is the maximum allowable value of ROCOF; and  $\Delta P_{\max}$  is the maximum value of generation loss that can be tripped from the network. It should be noted that  $S_{ESS,i}$  is the margin of ESS capacity, not the rated capacity of the ESS itself.

The primary frequency response support of ESS needs to be assessed along with the IR, to satisfy the steady-state operation constraint of the given network. The most important security constraint related to frequency is the under-frequency load shedding (UFLS). Generally, ESSs have a variable droop constant for frequency support, and it is considered in the target network, as shown in Fig. 3. According to (5), the minimum required droop constant can be calculated by assuming  $f_{\min}$  as the UFLS operating frequency.

$$\sum_{i=1}^m \frac{1}{R_{ESS,i}} \frac{S_{ESS,i}}{f_0} \geq \frac{\Delta P_{\max}}{f_{nom} - f_{\min}} - \sum_{i=1}^N \frac{1}{R_i} \frac{S_i}{f_0} \quad (11)$$

where  $f_{\min}$  is the minimum frequency of system requirement.

The primary frequency response support of the ESS is a temporary measure for contingency operation. Therefore, it is expected that the secondary or tertiary frequency response must be supported within some specified time. In general, the rebalancing of the network by automatic generation control or by the TSO takes at least 5 to 15 min [11]. From (4), the ESS primary frequency reserve requirement can be calculated in consideration of the secondary frequency response delay as:

$$\sum_{i=1}^m R_{ESS,i} \frac{S_{ESS,i}}{f_0} t_{hour} \geq S_{ESS,MWh} S_{SOC} \quad (12)$$

where  $S_{ESS,MWh}$  is the MWh capacity of the ESS;  $t_{hour}$  is the duration of the droop operation of ESS; and  $S_{SOC}$  is the SOC of the ESS.

The operation of the ESS can be optimized using (10), (11) and (12). As mentioned above (in Fig. 2), an ESS operation change will initiate the proposed methodology. First, the measured frequency data are used to track the maximum ROCOF after operation. The  $\sum H_i S_i$  value of the network can be calculated using (8). If this value is below the minimum required value, the optimal IR parameters of the ESS in the network are calculated and assigned to each ESS controller.

To minimize the effect of the proposed algorithm on the normal operation of the ESS, the operation point values of the PCS of ESS is considered for the calculation. The operation margin of the PCS capacity determines the variable  $S_i$  in (8) in the calculation of  $H_{ESS}$ . Because the capacity margin of the PCS in the ESS is altered continually, depending on the operation conditions,  $H_{ESS}$  is continuously assessed and modified.

Similarly, the primary frequency-support parameters are set in order to satisfy the grid operation conditions. In every iteration, the current ESS operation value is assessed to determine whether the margin of ESS capacity is sufficient to supply the required primary frequency support. If the required ESS capacity is not sufficient, the TSO can curtail or limit the operation bandwidth of the ESS.

### III. CASE STUDY

#### A. Simulation Data Construction

The simulation of frequency stability assessment was conducted based on an actual power system. Figure 4 depicts the transmission system of the Jeju island grid in Korea with six synchronous generators. Table I presents the detailed parameters of the facilities in the power system. As the penetration level of renewable generators increased, the displacement of synchronous generators continued until three must-run generators remained in the network, which was a crucial operation constraint to sustain the voltage of the power system. Prior to connecting each wind farm to the grid, the ESS substations aggregated their outputs and stepped up their voltages for main-grid connection. The capacity of an ESS was set to match a tenth of the capacity of the interconnected wind farms.

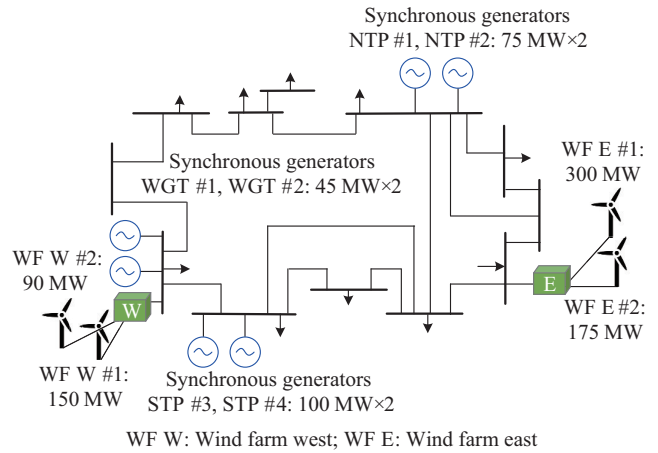


Fig. 4. Configuration of studied case.

TABLE I  
DETAILED PARAMETERS OF STUDIED CASE

Facility	Rated capacity (MW)	Droop constant	Governor type	Inertia constant (s)	Wind farm capacity (MW)
STP #3	100	0.05	IIEEG1	5.930	
STP #4	100	0.05	IIEEG1	5.930	
NTP #1	80	0.05	IIEEG1	6.000	
NTP #2	80	0.05	IIEEG1	3.735	
WGT #1	45	0.05	GAST2A	5.941	
WGT #2	45	0.05	GAST2A	5.941	
WF W #1					150
WF W #2					90
ESS west					25
WF E #1					300
WF E #2					175
ESS east					50

Note: Load demand is 708 MW.

#### B. Assessment of Frequency Stability

As the first step of simulation, it was assumed that the synchronous generators matched the supply and demand in the system, while four large wind farms supplied active power without curtailing their outputs. Each ESS substation smoothed out the volatility of production from the interconnected wind generators. During operation, the active power reference of the ESS substation was changed because of a decrease in the wind farm production in the network, as shown in Fig. 5. The frequency was measured and the grid stability was assessed at the time of the event, and optimal parameters were calculated based on the algorithm presented in Fig. 2. The measured frequency was transformed to the ROCOF value by polynomial approximation. The maximum ROCOF value was employed for calculating the inertia constant parameter using (8) and (10).

Table II shows the detailed simulation case parameters prepared in order to verify the proposed algorithm. For each scenario, the number of generators was planned to vary from six to four. The scenarios were designed to displace synchronous generators continuously as the renewable participation

in the network increased. The load demand remained constant while WGT #1 and WGT #2 disengaged gradually.

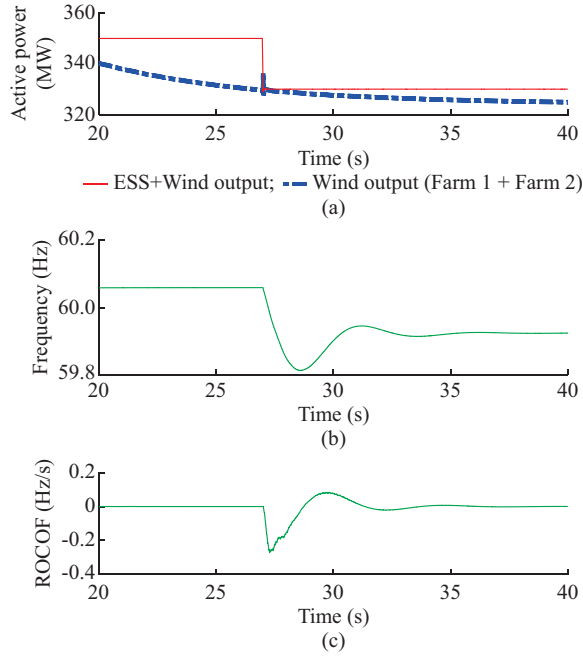


Fig. 5. Frequency response due to change of active power reference of ESS. (a) Output power of wind farm smoothed by ESS. (b) Grid frequency. (c) ROCOF.

TABLE II  
SIMULATION CASES FOR OPTIMAL PARAMETER CALCULATION OF ESS

Case	Number of generators	$\Delta P$ (MW)	ROCOF (Hz/s)	$f_0$ (Hz)
1	6	20	0.215	60.03
2	5	20	0.239	60.05
3	4	20	0.272	60.05

When a small step change was induced in the active power reference in the power system by the ESS, the change in frequency was measured to calculate the ROCOF and system stability parameters depicted in Table III. As the number of generators decreased, the sum of products of  $H_i$  and  $S_i$  declined eventually.

TABLE III  
SIMULATION RESULT FOR STABILITY ASSESSMENT IN EACH CASE

Case	$\sum H_i S_i$ (MJ)	$\sum H_{ESS,i} S_{ESS,i}$ (MJ)	ESS east margin (MW)	ESS west margin (MW)
1	2792	800	20	40
2	2512	1080	29	50
3	2208	1384	25	50

Simultaneously, information about the capacity margin of each ESS was also transferred to the grid operator. Using the parameters listed in Table III, the optimized frequency response parameters  $K_{IR}$  and  $R_{ESS}$  could be calculated as shown in Table IV and Table V, respectively. Prior to setting the parameters according to the optimized values, the maximum

frequency response values had to be compared with the ESS capacity margins.

TABLE IV  
OPTIMIZED IR PARAMETERS FOR EACH ESS

Case	$H_{ESS}$	$K_{IR}$	Maximum IR of ESS east (MW)	Maximum IR of ESS west (MW)
1	13.4	0.44	4.4	8.9
2	13.7	0.46	6.6	11.4
3	18.5	0.62	7.7	15.4

TABLE V  
OPTIMIZED DROOP CONSTANTS FOR EACH ESS

Case	$R_{ESS}$	Maximum IR of ESS east (MW)	Maximum IR of ESS west (MW)
1	0.0075	17.77	8.88
2	0.0085	11.92	14.39
3	0.0082	11.92	14.39

To confirm the parameters shown in Tables IV and V, a contingency scenario that tripped the largest generator in the grid was considered. According to the curves shown in Fig. 6, it could be deduced that the frequency of the grid was stable over the specified range.

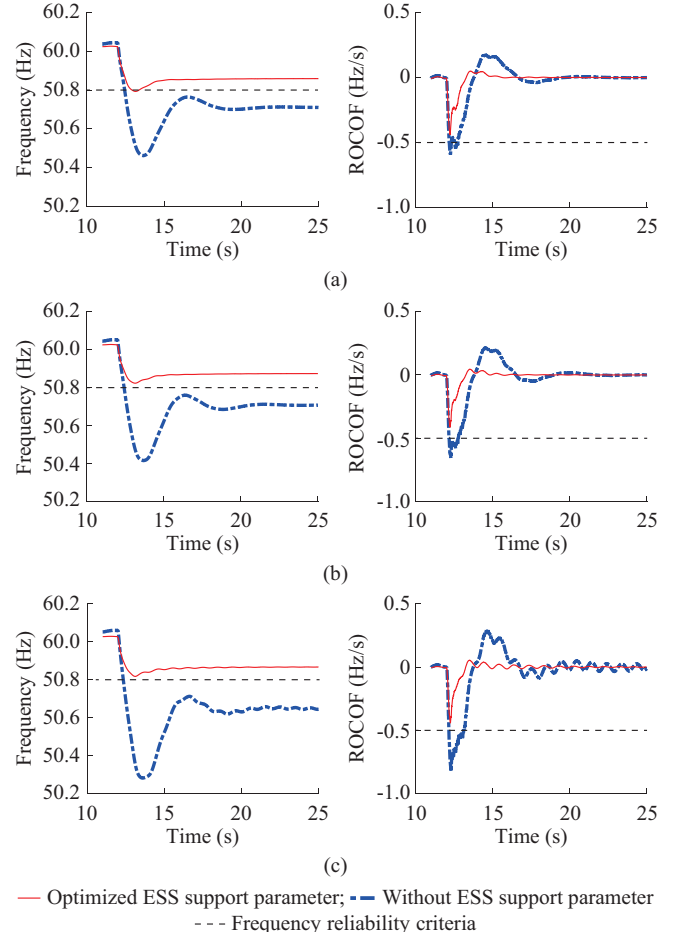


Fig. 6. Frequency and ROCOF after STP #3 tripping in different conditions. (a) With six generators. (b) With five generators. (c) With four generators.

As mentioned previously, the parameters listed in Tables IV and V were calculated based on two criteria for frequency stability: the steady-state frequency of the system after the contingency scenario, and the maximum value of RO-COF during the event. In the case of each simulation, the steady-state frequency remained above 59.8 Hz, which was a deviation of 0.2 Hz from the nominal frequency of the system. During the entire simulation, the absolute value of RO-COF appeared to be less than 0.5 Hz/s, owing to the modification of parameters.

The required ESS capacity was minimized to promote the maximum utilization of ESS within its original purpose such as load shifting or smooth-out operation. It should be noted that when adopting a calculated parameter for the ESS frequency support feature, the maximum IR and droop response from the ESS must not exceed the ESS operation margin. If both ESSs in the system are in the discharging mode, the operation margin of the ESS can be expected to decrease under the maximum IR and droop response quantities. In this case, the grid operator should implement an ESS limit, or additional generators should be dispatched in the system to maintain the stability of the network.

#### IV. CONCLUSION

This paper presented an ESS frequency stability assessment algorithm and operation strategy for a power system with high penetration of renewable generators. The contributions of the proposed method can be listed as follows:

1) An assessment of the system capability in the event of an operation parameter change in the ESS was conducted. The proposed method was found to be effective against large wind farm interconnection in grid with high penetration of renewable generators, as the change in the output caused by wind-source variability was small enough to be compensated for by the small ESS capacity in 15 to 30 minutes [2].

2) A method was proposed to determine the minimum requirement of the ESS operation point in any given situation. As shown in Table II, the operation limit of the ESS margin was calculated and compared with the actual margin value.

The assessment of system reliability is important in systems with high renewable penetration, because the participation of each generator varies as the renewable output changes. Using the proposed method, the TSO can assess the IR and primary frequency response reserve in a relatively short time. In the studied cases, the penetration levels of renewable generators varied from 60% to 74%. For each penetration level, the optimal ESS parameters were assessed and studied under the assumption of a worst-case scenario.

#### REFERENCES

- [1] REN21. (2018, Feb.). "Renewables 2018 global status report," [Online]. Available: <http://www.ren21.net/gsr-2018/>
- [2] H. Hannele, P. Meibom, C. Ensslin *et al.*, "Design and operation of power system with large amounts of wind power," IEA Wind Task 25, VTT Technical Research Center, Vuorimiehentie, Finland, Sept. 2006.
- [3] W. Ye, B. Herman, G. Maria *et al.*, "Method for assessing available wind primary power reserve," *IEEE Transaction on Sustainable Energy*, vol. 6, no. 1, pp. 272-280, Jan. 2015.
- [4] Nordel. (2007, Mar.). "Nordic grid code 2007," [Online]. Available: <https://www.entsoe.eu>
- [5] K. V. Vidyannandan and S. Nilanjan, "Primary frequency regulation by deloaded wind turbines using variable droop," *IEEE Transactions on Power Systems*, vol. 28, no. 2, pp. 837-846, May 2013.
- [6] R. U. Nayeem, T. Torbjorn, and K. Daniel, "Temporary frequency control support by variable speed wind turbines potential and application," *IEEE Transactions on Power Systems*, vol. 23, no. 2, pp. 601-612, May 2008.
- [7] J. B. Ekamayake, N. Jenkins, and G. Strbac, "Frequency response from wind turbines," *Wind Engineering*, vol. 32, no. 6, pp. 537-586, Dec. 2008.
- [8] Y. Wang, J. Meng, X. Zhang *et al.*, "Control of PMSG-based wind turbines for system inertial response and power oscillation damping," *IEEE Transaction on Sustainable Energy*, vol. 6, no. 2, pp. 565-574, Apr. 2015.
- [9] W. He, X. Yuan, and J. Hu, "Inertia provision and estimation of PLL-based DFIG wind turbines," *IEEE Transactions on Power Systems*, vol. 32, no. 1, pp. 510-521, Jan. 2017.
- [10] K. Vaclav, K. Sanjay, T. Remus *et al.*, "Sizing of an energy storage system for grid inertial response and primary frequency reserve," *IEEE Transactions on Power Systems*, vol. 31, no. 5, pp. 3447-3456, Sept. 2016
- [11] J. H. Eto, J. Undrill, P. Mackin *et al.*, "Use of frequency response metrics to assess the planning and operating requirements for reliable integration of variable renewable generation," Berkeley National Laboratory, University of California, California, USA, Apr. 2010.
- [12] P. M. Anderson and A. A. Fouad, *Power System Control and Stability*, 2nd ed. Hoboken, USA: Wiley InterScience, 2003.
- [13] ENTSO-E. (2018, May). "Rate of change of frequency (RoCoF) withstand capability: ENTSO-E guidance documentation for national implementation for network codes on grid connection," [Online]. Available: <https://www.entsoe.eu>
- [14] ENTSO-E. (2013, Apr.). "Supporting document for the network code on operational security," [Online]. Available: <https://www.entsoe.eu>
- [15] I. Toshio, T. Haruhito, Y. Kiyoshi *et al.*, "Estimation of power system inertia constant and capacity of spinning reserve support generators using measured frequency transients," *IEEE Transactions on Power Systems*, vol. 12, no. 1, pp. 136-143, Feb. 1997.
- [16] EirGrid. (2016, Mar.) "ROCOF alternative & complementary solutions project," [Online]. Available: <http://www.eirgridgroup.com/site-files/library/EirGrid/RoCoF-Alternative-Solutions-Project-Phase-2-Report-Final.pdf>

**Yeuntae Yoo** received the B.S. degree in electrical engineering from Korea University, Seoul, Korea, in 2013. He is currently pursuing the Ph.D. degree in electrical engineering at Korea University, Seoul, Korea. His research interests include renewable energy integration, power system stability and economic assessment of renewable generators.

**Seungmin Jang** received the B.S., M.S., and Ph.D. degrees in electrical engineering from Korea University, Seoul, Korea. He worked in the School of Electrical Engineering at Korea University, Seoul, Korea, as a Research Professor for 7 months. Since 2017, he has been with the Department of Electrical Engineering, Hanbat National University, Daejeon, Korea, where he is an Assistant Professor. His research interests include renewable energy resources and energy management system.

**Gilsoo Jang** received the B.S. and M.S. degrees in electrical engineering from Korea University, Seoul, Korea, in 1991 and 1994, respectively, and the Ph.D. degree in electrical and computer engineering from Iowa State University, Ames, USA, in 1997. He was a Visiting Scientist with Iowa State University, Ames, USA from 1997 to 1998 and a Senior Researcher with the Korea Electric Power Research Institute, Daejeon, South Korea, from 1998 to 2000. He is currently a Professor with the School of Electrical Engineering, Korea University, Seoul, Korea. His research interests include power quality and power system control.